MRS Communications (2019), *9*, 1151–1167
© Materials Research Society, 2019
doi:10.1557/mrc.2019.122

MRS Communications

Prospective Article

Redox-active polymers (redoxmers) for electrochemical energy storage

Mengxi Yang†, Chemical Sciences and Engineering Division, Argonne National Laboratory, Lemont, IL 60439, USA; Joint Center for Energy Storage Research, Argonne National Laboratory, Lemont, IL 60439, USA
Kewei Liu† and **Ilya A. Shkrob,** Chemical Sciences and Engineering Division, Argonne National Laboratory, Lemont, IL 60439, USA
Chen Liao, Chemical Sciences and Engineering Division, Argonne National Laboratory, Lemont, IL 60439, USA; Joint Center for Energy Storage Research, Argonne National Laboratory, Lemont, IL 60439, USA

Address all correspondence to Chen Liao at **liaoc@anl.gov**

(Received 19 July 2019; accepted 28 August 2019)

Abstract

Polymer redox-active materials (redoxmers) have numerous applications in the emerging electrochemical energy storage systems due to their structural versatility, fast-cycling ability, high theoretical capacity as electrode materials, sustainability, and recyclability. This review examines recent developments in improving the cycling performance of such materials and provides a vista on the future research directions.

Introduction

Energy consumption is increasing as the world economy grows. Based on the US Energy Information Administration's outlook from 2018, it is estimated that the global consumption will increase from 610 Quads (10^{15} British thermal units) in 2020 to 739 Quads in 2040.[1] Fossil fuels will remain the main energy resources in the coming decades. Currently, about two-thirds of the oil is used in transportation, and the climate change due to such massive CO_2 emissions can lead to economic and political turmoil.[2] Renewable energy sources, such as wind, tide, and solar, provide a less hazardous alternative; however, due to their intermittent nature, electrochemical energy storage systems (EESs) are needed to match the energy supply and demand over time. Such energy storage systems are already affecting our daily lives, and the systems with increased energy density and lower costs are in great demand.

The EES systems can be divided into two categories based on their applications: transportation energy storage and grid energy storage. Due to similar materials selection criteria, the research in transportation energy storage is mainly limited to concepts and chemistries that are already established in the industry, such as the $LiCoO_2$/graphite chemistry for lithium-ion batteries (LIBs). Since its commercialization in 1991 by SONY, $LiCoO_2$ (LCO) is still the most common cathode material found in consumer electronics. Since cobalt is relatively expensive and crustally scarce, the US Department of Energy has funded research projects to explore a sustainable and affordable alternative to the cobalt oxide cathodes, as the immense scale of grid storage makes reliance on unsustainable and expensive materials problematic. Few materials can compete with organic materials in the affordability; hence, there is a surging interest in substituting inorganic electrode materials with organic materials.

The grid energy storage is different, as it mainly provides arbitrage to dispatch intermittent energy generation to electric energy storage. Common examples of grid EES include redox flow batteries, including Zn–Cl, Zn–air, Zn–Br, and vanadium redox chemistries, and certain LIBs and lead–acid batteries.[3] Due to limited space of this review, these flow batteries will not be discussed, even though it is a rapidly growing field.

Here, we focus on solid macromolecular redox-active battery materials, with a brief section on supercapacitors (SCs). As shown in Fig. 1, a basic battery design includes the cathode, the anode, and the electrolyte which can be either solid or liquid. The cathode is a porous matrix consisting of micro- or nanoparticles of redox-active materials, conductive materials (that provide electron transport from the active materials, where charge separation occurs, to the metal current collectors), binders, additives, etc. The "active material" refers to the material that interconverts electric and chemical energy during electrochemical cycling. The binders are adhesives holding other particles in the electrode matrix together, so the matrix can withstand volume changes in the active materials as they cycle. The most common binder for LIBs is polyvinylidene fluoride (PVDF). Polymers can also be used as gel electrolytes due to their good processability and compatibility with different electrode surfaces.

Importantly, polymers can be more than binders and electrolytes: they can also serve as *active* materials. The use of organoradical, organo-sulfur, and carbonyl complexes for this purpose

† Both authors contributed equally.

https://doi.org/10.1557/mrc.2019.122 Published online by Cambridge University Press

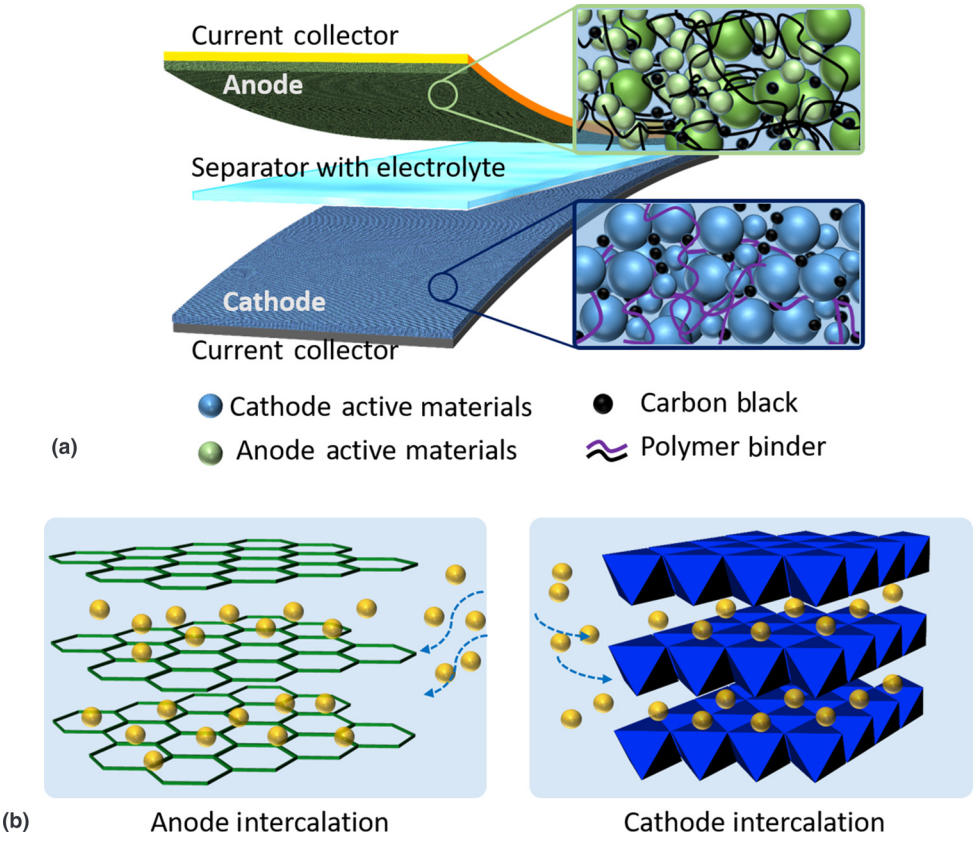


Figure 1. (a) Schematic representation of a battery and its components. (b) Ion intercalation into the electrodes, and the formation of SEI and CEI.

has been extensively reviewed.[4–6] Advantages of using *polymers* as battery materials include the ease of property/structure tuning by changing functional groups in the monomers, wide electrochemical stability windows, and greater safety. Using the term recently coined by Prof. Jeffrey S. Moore of the University of Illinois, we will refer to such redox-active polymer materials as redoxmers.

Our review is divided into sections by the application of redoxmers in different EES devices: lithium metal batteries (LMBs), sodium metal batteries (SMBs), magnesium metal batteries (MBs), lithium–sulfur (Li–S) batteries, SCs, and all-organic batteries. A very brief introduction to battery and polymer chemistry precedes this survey. In the final section, a perspective is given on the development of high energy density materials with improved sustainability and recyclability. The latter two properties are paramount for a wider EES use due to the global scale of electric grid storage.

This review is not intended to be comprehensive; rather, we intend it to be illustrative of the main developments in the field. In the following, we emphasize the electrochemical performance of the redoxmers, and the reviewed literature is limited to articles published after 2016 with a few exceptions. An overview of the cell performance of polymeric redoxmers is given in Table I at the end of this review.

Batteries and polymers: a brief introduction

Fundamentals of metal-ion batteries

In order to understand the functionality and application of polymer materials in EES devices, it is important to understand the basics of the solid-state battery design. LIBs (which are the most familiar example of such cells) shuttle Li^+ ions back and forth between the cathode and the anode. Initially, all "active" lithium (that is, the lithium that can be electrochemically cycled) is contained in a transition metal oxide cathode, such as LCO, where the Li^+ ions are intercalated between stacked two-dimensional (2D) layers of CoO_6 octahedra. The cathode is separated from the anode by a microporous polymer membrane (known as the separator), which is wetted by a liquid electrolyte. The electrolyte is an organic solution containing 1–1.5 M lithium salt, typically $LiPF_6$. During the charge process, the Li^+ ions leave the LCO lattice (this process is known as the deintercalation) and migrate across the pores in the electrode matrix and the separator into the graphite particles in the anode. In the discharge, lithium ions deintercalate from lithiated graphite and intercalate back into the cathode. As the lithium intercalates between the graphene sheets in graphite, the anode potential decreases to ~0.1 V versus Li/Li^+, and the surface becomes strongly reducing. The electrolyte exposed to this

https://doi.org/10.1557/mrc.2019.122 Published online by Cambridge University Press

https://doi.org/10.1557/mrc.2019.122 Published online by Cambridge University Press

TABLE I. Cell performance of polymeric redoxmers in energy storage.

Battery component	Redoxmer	Average discharge voltage (V)[a] (counter electrode)	Discharge capacity (mAh/g)	Discharge rate	Cycle number	Capacity retention (%)	Ref.
LMB electrode	P14AQ	2.14 (Li/Li^+)	260	2 C	1000	99.4	[7]
				20 C	20	69	
	P15AQ	2.09 (Li/Li^+)	260	C/5	100	67.6	[7]
	PNMe	2.5 (Li/Li^+)	138	10 C	1000	90	[8]
				20 C		70	
	PNAn	2.5 (Li/Li^+)	119	1 C	500	98	[9]
				10 C		80	
	PNNO	2.5 (Li/Li^+)	93	10 C	500	80	[9]
	PDI-Tc	2.5 (Li/Li^+)	75.9	C/2	200	88.2	[10]
	P(TMA-co-TFSI)	3.67 (Li/Li^+)	~20	30 C	100	83	[11]
	P1	3.6 (Li/Li^+)	106	50 C	1000	>90	[12, 13]
	PV10	−1 ($TEMPO/TEMPO^+$)	–	–	–	–	[14]
	Poly(Te-BnV)	−2.67 ($TEMPO/TEMPO^+$)	502	100 mA/g	50	89	[15]
LMB binder	P(EDOT-TEMPO)	N/A	–	–	–	–	[16]
LMB electrolyte	Polysterene-Li^+-TFSI	N/A	–	–	–	–	[17]
LMB additive	Poly-EC, poly-VC	N/A	–	–	–	–	[18, 19]
LMB interface	PEDOT	N/A	–	–	–	–	[20]
SMB electrolyte	THEICTA	–	–	–	–	–	[21]
SMB electrode	Poly(S-PETEA)	~1.3 (Na/Na^+)	877	C/10	60	91.4	[21]
	P2	1.6 (Na/Na^+)	150	C/10	25	40	[22]
	PAN	1.6 (Na/Na^+)	350	C/10	75	53	[22]
	PMDA	1.5 (Na/Na^+)	185	23 mA/g	100	68	[23]
MB electrode	NP	1.7 (Mg/Mg^{2+})	85	2.5 C	–	70[b]	[24, 25]
	PAQS	1.6 (Mg/Mg^{2+})	100	30 mA/g	100	30	[26]
	P14AQ	1.6 (Mg/Mg^{2+})	133	C/2	105	99	[26]

Continued

https://doi.org/10.1557/mrc.2019.122 Published online by Cambridge University Press

TABLE I. Continued

Battery component	Redoxmer	Average discharge voltage (V)[a] (counter electrode)	Discharge capacity (mAh/g)	Discharge rate	Cycle number	Capacity retention (%)	Ref.
	P26AQ	1.5 (Mg/Mg^{2+})	122	C/2	100	82	[26]
	P(NDI2OD-T2)	1.5 (Mg/Mg^{2+})	54	50 C	–	70[c]	[27]
Li-S electrode	Poly(S-*r*-DIB)	~2.1 (Li/Li^+)	1100	C/10	100	75	[28]
	Poly(S-co-DiPhDY)	~2.3 (Li/Li^+)	800	C/5	850	300	[29]
	SIVHP	2.0 (Li/Li^+)	1248	C/10	400	~16	[30]
	PABTP	2.3 (Li/Li^+)	1500	40 mA/g	77	54	[31]
	Poly-C_6S_6	2.2 (Li/Li^+)	150	C/10	200	98	[32]
	SPAN[d]	~1.6 (Li/Li^+)	755	2C	900	81[e]	[33]
Supercapacitor	CNT	~3.5 (Li/Li^+)	210[f]	0.1–10 A/g	10^4	85	[34]
	FGH	~0.5 (Li/Li^+)	441[f]	10 A/g	10^4	86	[35]
All-redoxmer electrode	Poly (vinyldibenzothiophenesulfone)	−1.8 (Ag/AgCl)[g]	221	10 C, 120 C	100	>95	[36]
	PDB	3.4–1.5[h]	249[i]	1 A/g	250	48	[37]

[a]When no specific value was reported, the average discharge voltage was estimated from the voltage-capacity profiles.
[b]Compared to cycling at 0.25 C.
[c]Compared to cycling at 0.2 C.
[d]Loaded in the SBA-15 mesoporous template.
[e]Compared to cycling at 1 C.
[f]Unit in F/g.
[g]Potential of the dibenzothiophenesulfone monomer.
[h]Voltage of battery as assembled.
[i]Capacity of the full battery.

surface becomes decomposed forming a thin (<100 nm) layer of insoluble, electrically insulating material called the solid electrolyte interphase (SEI, Fig. 1). The SEI is a thin Li-ion conducting layer of products of electrolyte breakdown that prevents runaway reduction of the organic electrolyte by the lithiated graphite. The inner layer of the SEI is composed of fully mineralized species, such as LiF and Li_2CO_3 crystallites, while the outer layer consists of partially reduced, polymerized material derived from the organic solvent. Similarly, the cathode electrolyte interphase (CEI) is formed by oxidation of electrolyte on the energized (delithiated) surface of a cathode (Fig. 1). Both interphases stabilize the cell by shielding the reactive surfaces from the organic molecules in the electrolyte; it is essential that while doing so, these interphases can rapidly conduct Li^+ ions but entirely block electron and molecular transport.

The SEI played a pivotal role in the development of LIB technology. Before the introduction of commercial LIBs in 1991, there were already numerous LIB prototypes, but their safety and performance were wanting. Replacement of lithium metal by lithiated graphite and the discovery of a "magic" SEI-forming electrolyte were important milestones on the path to commercialization. Akira Yoshino discovered that ethylene carbonate, a polar solvent with high oxidative stability on the LCO cathode, formed a stable SEI on lithiated graphite, and the rest was history.

Most of the batteries considered in this review do not have the graphite anode that is used in the commercial LIBs. Lithiated graphite (LiC_6) is an exceptionally stable material with small (<10%) volume expansion, but it has a relatively low energy density. The high volumetric capacity for metal anodes (3832 mAh/cm^3 for Li and 2017 mAh/cm^3 for Mg) can significantly improve the energy density of storage. In the Li metal anode batteries, reduced lithium ions become part of the anode. This leads to many challenges, as continuous remodeling of the Li surface during lithiation and delithiation yields unstable SEI, and is also accompanied by a growth of lithium dendrites (spiny protuberances grown from the surface). The dendrites are especially problematic, as they can grow across the separator and short the battery, resulting in a thermal explosion. The dendrites are known to grow both on lithium and sodium, but not on magnesium. However, unlike the alkali ions, the divalent Mg^{2+} ion cannot migrate through passivation layers containing MgO or $MgCO_3$. Thus, it is imperative to keep the Mg surface clean of all residues that block ion transport across the interphase.

As a cell ages over many charge/discharge cycles, the discharge capacity decreases with each cycle, and the battery is slowly "dying." This decrease is caused by parasitic reactions that include the formation of SEI and other electrode deposits, loss of the active material, loss of electric connectivity between the particles in the electrode matrix, amorphization, pulverization of the active particles, chemical and morphological changes in the electrodes, and acid corrosion. As a characteristic of battery cyclability, the cells are galvanostatically cycled at a constant current rate, and the ability to maintain discharge capacity over a set number of cycles at a fixed rate is referred to as the capacity retention. The resulting capacity is typically reported as specific capacity per weight of active material. The specific capacity can be considerably lower than the theoretical capacity, which is estimated from the known or assumed energy density of active materials in the electrodes. During cycling, the cell voltage is limited between the lower cut voltage (LCV) and upper cut voltage (UCV). If the voltage exceeds UCV, there could be oxidation of electrolyte resulting in rapid loss of capacity. Due to the formation of resistive films on the electrodes, the finite rate of ion diffusion through the active particles, the tortuosity of channels in the electrode matrices, and the depletion of ions in the electrolyte, all batteries have internal resistances (impedances) that cause the cell voltage to increase more rapidly as a function of capacity for higher currents. For LIBs, operation at rates >1–3 C (where 1 C corresponds to full charge in 1 h) results in numerous problems, whereas fast charging at rates of 6–8 C is greatly desired by the industry and consumers. Surpassing such limitations is one of the main reasons to replace inorganic electrodes with polymer materials.

Fundamentals of polymers

We remind that a polymer consists of multiple repeating units called monomers, with its origin from Greek *πολυμερές*, which means having many parts. As indicated by this name, polymers have a high molecular weight (MW). These macromolecules can be classified as either condensation or addition polymers based on the synthetic method (fusion of functional groups or sequential addition of monomers, respectively). The chains formed by covalently linked monomer units are the backbone of the polymer, and the groups to the side of this backbone are pendant groups. The redox-active moieties can be in the backbone or these pendant groups depend on the polymer design. Their morphology can change from linear to branched to hyperbranched to dendritic, and more structural types are available when different polymer chains are joined together in copolymers. This structural and morphological versatility is the chief attraction of the polymers to a battery scientist.

With these preliminary considerations in mind, we begin our survey of different EES devices, starting with the familiar lithium batteries.

Lithium metal batteries

A common goal of the electrode development for LMBs is to replace LCO with inexpensive and crustally abundant active materials. Furthermore, cycling of redoxmers releases less heat compared to Li-ion insertion into transition metal oxides, resulting in faster and safer battery charging.[5]

Electrode

The redoxmers in the electrodes can be divided into (i) conjugated polymers whose conductivity and redox properties

https://doi.org/10.1557/mrc.2019.122 Published online by Cambridge University Press

depend on doping and (ii) polymers with redox-active functional groups that include carbonyls, *N*-oxyls, and aromatic heterocycles. The small-molecule analogs of redoxmers including such groups are, respectively, the quinones, (2,2,6,6-tetramethylpiperidin-1-yl)oxyl radical (TEMPO) and viologen dications.

Taking anthraquinone (AQ) as an example, at 2.26 V versus Li/Li^+, a neutral molecule in a carbonate electrolyte can accept two electrons to form a lithiated dianion (Li_2AQ).[7] While this reaction is fully reversible, the neutral and charged monomers can migrate out of the electrode matrix, causing irreversible capacity loss. Immobilization of the redox-active moieties in a long-chain insoluble polymer addresses this concern. For example, by using a one-step condensation reaction, Zhou and coworkers synthesized high-MW poly(1,4-anthraquinone) (P14AQ, ~230 kDa) shown in Fig. 2.[7] The theoretical specific energy for this material is 560 versus 530 Wh/kg for LCO. In the cell, this P14AQ cathode exhibited 99.4% discharge capacity retention after 1000 cycles at a rate of C/5 (=full charge in 5 h). In comparison, AQ-containing cathode retained only 18% of the initial discharge capacity after 100 cycles. A lighter polymer, poly(1,5-anthraquinone) (P15AQ) with MW

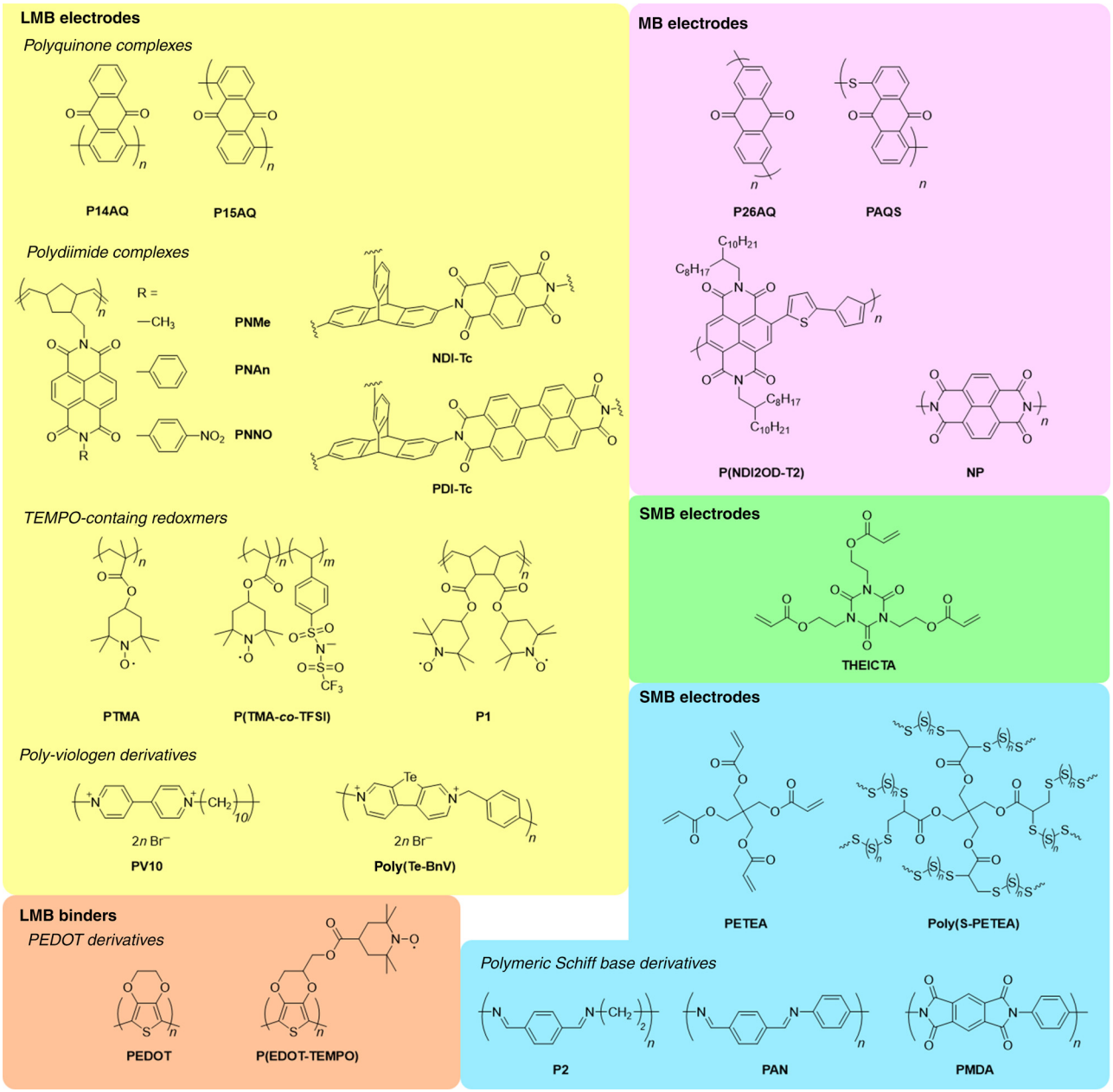


Figure 2. Redoxmers for EES surveyed in this review.

https://doi.org/10.1557/mrc.2019.122 Published online by Cambridge University Press

~2.3 kDa, retained ~68% capacity after 100 cycles. The correlation between the MW and capacity retention indicates that immobilization is required for preventing a gradual loss of the active material. Apart from the improved capacity retention, the cathode-containing high-MW P14AQ retained 69% capacity at a rate of 20 C. As will be shown, this exceptional fast-cycling ability is typical for many other redoxmer cathodes.

The downside of having insoluble redoxmers are complications arising in the manufacture of electrode laminates that are typically processed from thick liquid slurries.[5] An alternative approach is including the redox molecules as pendant groups, which makes for a more flexible and hence more soluble polymer. Nishide and coworkers reported several such polymers containing naphthalene diimide (NDI) pendants on a polynorbornene backbone (Fig. 2).[8] Heterocyclic pendants such as perylene diimide (PDI) and NDI undergo reversible two-electron redox reactions at ~2.5 V versus Li/Li^+, and their polymers can be charged and discharged as rapidly as P14AQ. Methylated-derivative PNMe (Fig. 2) maintained 70% of the initial capacity when cycled at a rate of 20 C,[8] and PNAn and PNNO also shown in Fig. 2 demonstrated >80% capacity retention at a rate of 10 C. PNAn also shows long-term stability, maintaining 98% theoretical capacity over 500 cycles at 1 C.[9]

Importantly, redoxmer architecture is not limited to linear chains. For example, Seferos and coworkers incorporated the diimides into a triptycene-based three-dimensional organic framework (Fig. 2).[10] For PDI-Tc, this framework had a long-range order, whereas for NDI-Tc, it was less ordered. This morphology difference affects cathode properties. In the cathode matrix, NDI-Tc forms irregular, nonconductive aggregates resulting in inferior battery performance, while PDI-Tc electrodes retain 80% capacity with nearly 100% Coulombic efficiency after 500 cycles at a rate of 2 C. For comparison, for the *monomer* PDI introduced into the same electrode matrix, only 7.5% capacity remained after 500 cycles, demonstrating the importance of redoxmer immobilization.

Since the redoxmers used in cathodes all have their redox potentials in a limited range between 2 and 4 V versus Li/Li^+, their specific capacity is greatly affected by MW of the polymer. Among the examples considered above, backbone-type polymers have a greater specific capacity than pendant-type polymers. For example, theoretical capacity of PNAn (Fig. 2) is 120 mAh/g,[9] while for the PDI-Tc framework it is only 76 mAh/g.[10] Nonetheless, as it is convenient to introduce redox-active groups as pendants, one option for increasing the power density is to use the pendant groups with higher redox potentials, such as *N*-oxyls.

The most commonly used compound of the *N*-oxyl kind, TEMPO, has the redox potential of ~3.6 V versus Li/Li^+. Numerous studies of TEMPO redoxmers have been reported since their debut in 2002.[38] The redoxmer used in that original study, poly(2,2,6,6-tetramethylpiperidinyl-oxymethacrylate) (PTMA, Fig. 2), was synthesized by radical polymerization of the piperidine-based precursor, followed by oxidation of the product. PTMA is still being optimized. To speed up Li^+ ion migration into the polymer during cycling, Nishide and coworkers synthesized a copolymer consisting of PTMA and trifluoromethanesulfonylimide ($TFSI^-$), P(TMA-*co*-TFSI) (Fig. 2).[11] In this copolymer, the $TFSI^-$ anions are paired with Li^+ ions that migrate along the polyanion chains. While the theoretical capacity of this copolymer (48 mAh/g) is lower compared to PTMA (111 mAh/g), the incorporation of $TFSI^-Li^+$ conduits into this polymer obviates the need for liquid electrolyte thereby improving the overall cell capacity and safety (by the elimination of flammable organic liquids). During discharge, TEMPO oxidizes to an *N*-oxoammonium cation that pairs with the $TFSI^-$ anion; the latter releases the Li^+ counter ion. A comparison of P(TMA-*co*-TFSI) with the PTMA/PTFSI composite suggests that almost all TEMPO pendants in the copolymer participate in the redox reaction. As a result, this copolymer can be cycled at a rate of 30 C reaching the upper cell voltage of 3.7 V.

In addition to the polyacrylates, TEMPO pendants can be grafted onto polynorbornene backbones. A TEMPO-substituted polynorbornene P1 shown in Fig. 2 was prepared via esterification of the dicarboxylic anhydride monomer.[12] Degenerate electron transfer occurring during charging of P1 was studied in detail.[13] The authors observed the occurrence of electron hopping between TEMPO groups in different states of charge and quantified the effect of the solvent on the rate of this self-exchange.

Lastly, aiming at *all*-organic radical LIBs, several research groups have considered the *anode* redoxmers. One such design includes the viologen (1,1′-diethyl-4,4′-bipyridinium) dication and its derivatives. This dication undergoes two consecutive one-electron reductions to yield a neutral molecule. A common viologen redoxmer, PV10 (poly(N-4,4′-bipyridinium-*N*-decamethylene dibromide) shown in Fig. 2, has the redox potential that is 1 V lower than TEMPO.[14] To decrease the redox potential further, He and coworkers introduced group-6 heteroatoms (S, Se, and Te) into the viologen backbone.[6,15] The resulting heterocyclic redoxmer [poly(Te-BnV), Fig. 2] has the redox potential that is 2.67 V lower than TEMPO. When loaded on single-walled carbon nanotubes (CNTs), this anode material achieved a reversible capacity of 502 mAh/g at the current density of 100 mA/g with the Coulombic efficiency ~100%.

Binders

Introducing redox-active groups to conductive polymer binders not only adds capacity but also facilitates charge channeling and improves polymer solubility. To illustrate, Armand and coworkers reported a modification of the commonly used the conductive binder poly(3,4-ethylenedioxythiophene) (PEDOT) with pendant TEMPO groups. The resulting multifunctional P(EDOT-TEMPO) polymer (Fig. 2) is soluble in acetonitrile. When it is used as a binder in $LiFePO_4$ cells and compared to conductive carbon additive and the conventional PVDF

https://doi.org/10.1557/mrc.2019.122 Published online by Cambridge University Press

binders, P(EDOT-TEMPO) provided the improved fast-cycling capability and higher Coulombic efficiency.[16]

Electrolyte

Redoxmers can double as electrolytes. A recent example of this functionality is a block copolymer containing (i) a polystyrene structural block, (ii) a Li-ion conducting block, and (iii) a functional block that includes poly(ethylene-alt-maleimide) doped with LiTFSI.[17] With ionic conductivity of 8×10^{-5} S/cm and a Li^+ ion transference number of 0.92 at 40 °C, this redox-active polymer provided a competitive alternative to redox-inactive solid-state polymer electrolytes.

Additive

The redoxmers can also serve as SEI and CEI modifiers. Electrolyte additives are used to improve the properties of SEI, by facilitating Li^+ ion conduction across this interphase without undermining its structural and chemical stability.[39] Given that outer SEI already consists of "naturally" occurring polymers generated by solvent reduction, researchers have intentionally introduced synthetic analogs of such redoxmers,[18,19] but the practical usefulness of this approach remains unclear.

Coating/interface

Redoxmers can modify the surface of the oxide particles in the cathode slowing down acidic corrosion, mitigating the impedance rise, and reducing transition metal-ion dissolution. While various inorganic films, including phosphates,[40] alumina,[41] fluoride, and oxyfluorides[42] have been considered as such coatings, more recently, conductive polymer coatings were also examined.[20] Xu et al. reported the protection of a high voltage cathode $LiMO_2$ (where M can be Ni, Co, or Mn) by infusing the oxide particles with a conductive PEDOT polymer using an oxidative chemical vapor deposition (oCVD) method shown in Fig. 3. This treatment increases capacity retention and improves thermal stability at high voltages.[20] We remind that such nickel-rich oxides are introduced as compound (secondary) particles consisting of multiple sintered crystal grains (primary particles). Even the pristine secondary particles have microscopic voids due to gas evolution during their synthesis; as the material becomes delithiated, cracks develop between the primary particles preventing their fast lithiation and delithiation. It was speculated that the PEDOT infused the secondary particles to facilitate charge transport between the primary particles. As illustrated in Fig. 3, the polymerization is induced by mixing of gaseous $VOCl_3$ and 3,4-ethylenedioxythiophene (EDOT), so the PEDOT coating is ultraconformally applied. This polymer can interfere with the cathode damage in more than one way, by binding corrosive acid, reacting with oxygen species released from the surface as the cathode becomes destabilized by delithiation,[43] or by improving thermal conductivity between the primary particles.

Sodium metal batteries

Due to the crustal abundance of sodium, large-scale Na-metal batteries (SMBs) are particularly attractive for the smart electric grid. While lithium and sodium are both alkali metals, SMB and LMB chemistries can be quite different. As Johnson and coworkers observed back in 2013,[44] though certain scientific and engineering knowledge translates from one chemistry to another, the research on sodium batteries is largely original.

Presently, there are many examples of redoxmers serving as SMB *cathodes*. Armand and coworkers reported a quasi-solid-state Na–S cell containing poly(*S*-pentaerythritoltetraacrylate (PETEA))-based cathode and a (PETEA-*tris*[2-(acryloyloxy) ethyl] isocyanurate (THEICTA))-based gel polymer electrolyte shown in Fig. 2.[21] The redoxmer was synthesized in a process similar to inverse vulcanization (see the section Inverse vulcanization below). The gel polymer electrolyte provides high Na^+ ion conductivity while blocking polysulfide anions that carry parasitic currents (see the section Lithium–sulfur batteries). The poly(*S*-PETEA) redoxmer strongly binds NaS_x salts from the electrolyte, shifting the ionic equilibria discussed in the section Lithium–sulfur batteries. This cathode delivered a high specific capacity of 877 mAh/g at a rate of C/10.

Fewer examples exist of the redoxmers serving as *anode* materials in SMBs. The most commonly used anode material in LIBs, graphite, is not size-compatible with the Na^+ ion, which causes irreversible intercalation.[44] Hard carbon has been used instead, but this material cannot be used at high rates. Redoxmers can address this concern. In 2014, Armand and coworkers reported two poly-Shiff bases serving as anode materials for SMBs (Fig. 2).[22] The anode reaction (~1.6 V versus Na^+/Na) involves the cationic insertion of sodium ion into reduced units. For nonconjugated P2, the capacity retention was poor, whereas for fully conjugated poly-[*N,N′-para*-(benzylidene)phenylenediamine] (PAN) the capacity was more stable. With sodium *bis*(fluorosulfonyl) imide in methyltetrahydrofuran as the electrolyte, a capacity of 350 mAh/g and stable cycling at a rate of 26 mA/g were demonstrated for the latter system. More recently, Zhao et al. reported the pyromellitic dianhydride (PMDA)-based polyimides,[23] which can be conveniently synthesized in hydrothermal reactions. PMDA accepts two electrons below 1.5 V versus Na/Na^+, and it showed a capacity of 125 mAh/g after 100 cycles. The development of such redoxmers presents opportunities to construct an all-organic cell that can be compatible with aqueous electrolytes.

Magnesium metal batteries

As energy-dense charge carriers, multivalent ions such as Al^{3+}, Ca^{2+}, and Mg^{2+} have many advantages over the more commonly used monovalent alkali ions. Magnesium, in particular, is easily mineable, and it makes an excellent anode in its metallic form. Indeed, the theoretical volumetric capacity of Mg metal (3832 mAh/cm^3) is significantly higher than that for Li metal (2046 mAh/cm^3). The main roadblock for

https://doi.org/10.1557/mrc.2019.122 Published online by Cambridge University Press

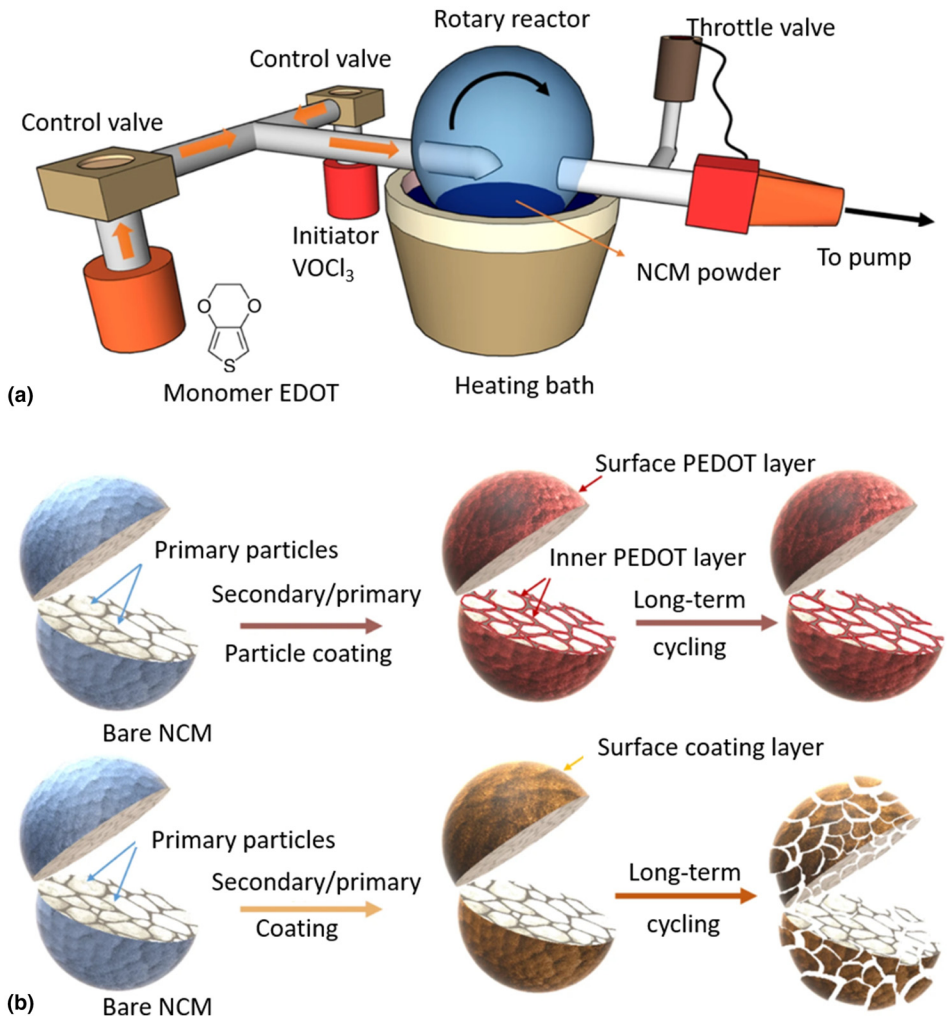


Figure 3. oCVD process. (a) Schematic diagram of the oCVD setup. The process relies on uniform vapor (oxidant and monomer) adsorption and subsequent in situ polymerization on the oxide particle. (b) The oCVD process led to conformal PEDOT coating of secondary and primary particles, resulting in no particle cracking after a long cycle life. Reproduced with permission from Ref. [20]. Copyright 2019, Springer Nature.

using this higher energy density is a paucity of suitable cathode materials, as reversible intercalation of Mg^{2+} ion into layered crystals (unlike that for Li^{+} ion) is uncommon. Slow migration of Mg^{2+} in solids and a large penalty for ion desolvation during a transition from the electrolyte to the cathode are also common concerns. The current state-of-the-art cathode for MBs is the Chevrel phase of Mo_6X_8, where X stands for a chalcogenide (S, Se, or Te). Uncommonly high mobility of Mg^{2+} ions in this material is attributed to weak interactions of Mg^{2+} with chalcogenide atoms in the crystal lattice. Certain thiospinels (such as Ti_2S_4) and ternary spinel chalcogenides[45] also have this property. Computer-assisted discovery of new materials[46] will bring more examples of such crystalline materials; however, the present scarcity gives the redoxmer cathodes a chance to redefine MB development. In all MB designs, Mg metal serves as the negative electrode.

Dominko and coworkers reported the use of naphthalene-hydrazine poly(diimide) (designated NP in Fig. 2) with Mg $(TFSI)_2$ in a mixture of tetraethylene glycol dimethyl ether and dioxolane serving as the electrolyte.[24] For this cell, the average discharge voltage was 1.7 V, and the Coulombic efficiency was 99%. The cathode operated at ~42% theoretical capacity, suggesting that two out of four carbonyls in the diimide unit became charged and discharged. *Operando* infrared spectroscopy was used to monitor redox reactions of these carbonyl groups during cycling of the cell.[25]

Liao and coworkers reported a polyanthraquinone (PAQ)-based cathode for MBs. Compared to 1,5-poly(anthraquinonylsulfide) (PAQS, Fig. 2) used in LMBs, poly-2,6-anthraquinone (P26AQ, Fig. 2) and poly-1,4-anthraquinone (P14AQ, Fig. 2) were found to be more stable at high rates.[26] In particular, P26AQ delivered 100 mAh/g discharge capacity after 100 cycles at a rate of C/2 with ~82% capacity

https://doi.org/10.1557/mrc.2019.122 Published online by Cambridge University Press

retention; for P14AQ, this capacity was 105 mAh/g after 100 cycles with 99% capacity retention. Importantly, the redox potential of P14AQ is 0.3 V versus the Chevrel phase Mo_6S_8 cathode, so this polymer material is already competitive with the best inorganic electrodes.

Charge storage by multivalent cations can be sensitive to solution chemistry.[27] This aspect is unique to the multivalent ions, and care needs to be exercised to avoid unwanted side reactions. For example, Yao and coworkers observed that a chloride-containing electrolyte led to mostly $MgCl^+$ uptake in the cathodes consisting of P14AQ and poly{[*N,N'*-bis (2-octyldodecyl)-1,4,5,8-naphthalenedicarboximide-2,6-diyl]-alt-5,50-(2,20-bithiophene)} (P(NDI2OD-T2) shown in Fig. 2, while a chloride-free electrolyte led to Mg^{2+} ion uptake, which is the preferred way of charge storage in the MBs.

Like in other batteries, the MB redoxmers can be used as electrolytes. Wallace and coworkers used crosslinking to obtain a hydrogel consisting of polypyrrole (PPy)/PEDOT as an electrolyte for Mg–air battery.[47] The high capacity (32 mAh/cm^2) and energy density (22 mWh/cm^2) in the corresponding cells were attributed to the microporous structure of this material. The same group reported a silk fibroin–chlorine nitrate electrolyte with a specific capacity of 0.06 mAh/cm^3.[48] Biodegradable redoxmers of this type can be used in transient medical bionics.

Lithium–sulfur batteries

In the last decade, rechargeable Li–S batteries have attracted attention due to their high energy density and low cost.[49,50] Paired with the Li metal, the sulfur cathode can deliver 2.15 V. Elemental sulfur has the theoretical lithium capacity of 1672 mAh/g, which per weight is 10 times greater than the capacity of transition metal layered oxides in LIBs.[51,52]

During discharge, S_8 undergoes a multistep reduction from soluble lithium polysulfides (S_x^- with $x = 4$–8) to insoluble Li_2S_2 or Li_2S salts. When the cell is charged, the insoluble lithium sulfide is oxidized back to the soluble lithium polysulfides and then to the elemental sulfur. While this chemistry is well understood, there are several issues that need to be addressed for the Li–S batteries to become competitive with LIBs. First, the low electric conductivity of elemental sulfur and lithium sulfide leads to excessive cell polarization. Second, the polysulfide anions shuttle between the electrodes carrying parasitic currents while undergoing side reactions.[53,54] Third, large volume change (to 80%) during cycling causes depletion of sulfur and capacity loss. Fourth, using Li metal anodes causes undesired behaviors already known from the LMBs, such as rapid dendrite growth and SEI destabilization on the Li surface.[55–57] Numerous strategies have been suggested to mitigate these effects that include the use of carbonaceous materials to encapsulate sulfur,[58] polar groups to bind sulfur chemically,[59] and solid electrolytes to stop polysulfide shuttling.[60] Redoxmers have also been explored as cathodes, binders,[61] electrode matrices,[62] and surface coatings[63]; here, we will concern ourselves with their use in the cathodes. Three major strategies to obtain polymer materials with high sulfur content have been pursued: the inverse vulcanization, the inclusion of sulfur into monomers, and the direct sulfurization.

Inverse vulcanization

The inverse vulcanization is a one-pot reaction introduced by Pyun and coworkers in 2013.[64] It has been demonstrated on the kilogram scale.[65] The general approach [Fig. 4(a)] is to copolymerize divinylic monomers (such as 1,3-diisopropenylbenzene, DIB) and sulfur chains. It is a visually arresting reaction: the yellow sulfur becomes converted to a dark-red poly(sulfur-random-1,3-diisopropenylbenzene). The latter delivers the specific discharge capacity of 1100 mAh/g with the capacity retention of 75% after 100 cycles. At 10 wt % DIB, still better capacity retention was reported (1005 mAh/g after 100 cycles and 817 mAh/g after 300 cycles) with the Coulombic efficiency of 99%.[28] Later on, Pyun et al. obtained the 1,4-diphenylbutadiyne (DiPhDY) polymer shown in Fig. 4(b), with a greater density of the disulfide bonds. The cathode containing 90 wt% sulfur delivered the discharge capacity of 800 mAh/g after 300 cycles at a rate of C/5 and lasted for 850+ cycles.[29] Other monomers, such as 1,3-diethynylbenzene,[66] limonene,[67] and 4-vinylpyridine,[68] have been considered. While these S-containing polymers are all insoluble, soluble redoxmers can be obtained through suitable branching. For example, Gao's group synthesized water-soluble inverse-vulcanized hyperbranched polymers (SIVHPs) by sequential thiol-ene click reactions and Menschutkin quaternization. The SIVHP-based cells exhibited the specific discharge capacity of 1248 mAh/g and lasted for 400 cycles.[30] To increase the conductivity of the cathode, Sung and Zentel combined sulfur and allyl terminated poly (3-hexylthiophene-2,5-diyl) (P_3HT) using Grignard metathesis polymerization. Their cathode showed improved fast-cycling properties with the specific discharge capacity of 740 mAh/g at a rate of 1 C.[66]

Sulfur-containing monomers

Redox-active S-containing monomers can be polymerized; during charging, the thiol groups in their units are converted to thiolate anions. In 1992, Jonghe and coworkers proposed the first material of this class, 2,5-dimercapta-1,3,4-thiadiazole (DMcT).[69] During discharge, this macromolecule depolymerized into a mixture of di- or trithiolates; during charge, the thiolate anions oxidized and formed a polymeric disulfide [Fig. 5(a)]. However, capacity retention was poor due to side reactions, so this material remained as an isolated example. It was subsequently realized that to avoid such depolymerization, sulfur can be introduced into *side* groups of the polymer. To give an example, a sulfur-containing monomer, anthra [1,9,8-b,c,d,e][4,10,5-b,c,d,e]bis-[1,6,6a(6a-S)trithia]pentalene (ABTP), was synthesized from anthracene.[31] By oxidative coupling of this monomer, a ribbon-like polyanthra[1,9,8-b,c,d,e][4,10,5-b,c,d,e]bis-[1,6,6a(6a-S)trithia]pentalene (PABTP)

https://doi.org/10.1557/mrc.2019.122 Published online by Cambridge University Press

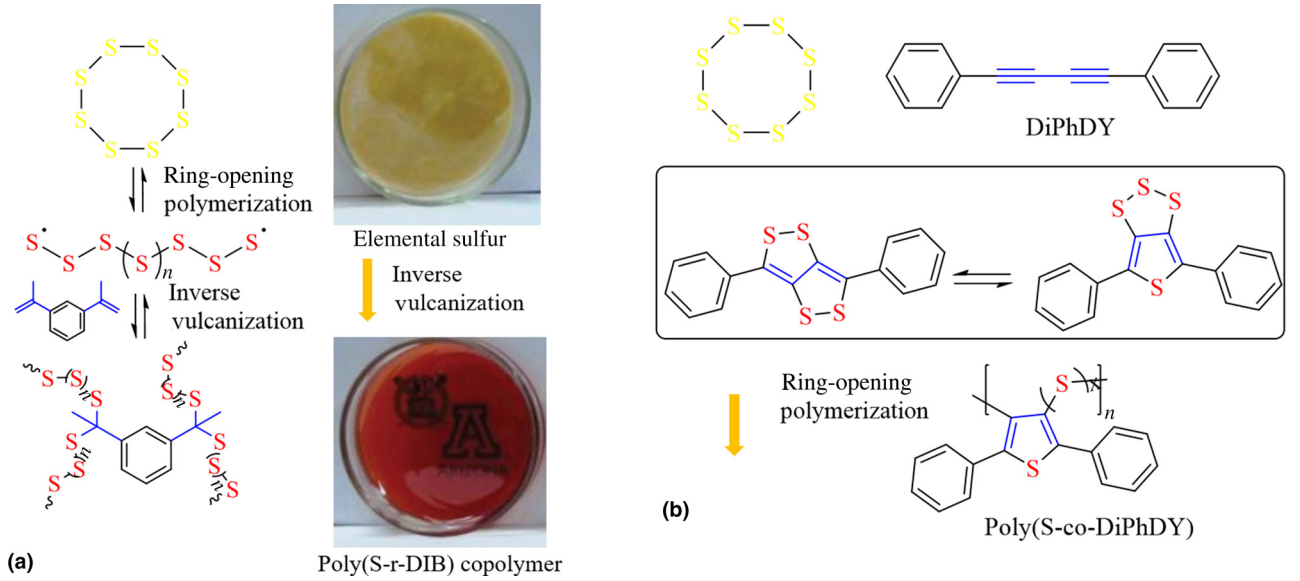


Figure 4. (a) Schematic illustration of the synthesis of poly(S-r-DIB) via inverse vulcanization. The photos are used with permission from with permission from Ref. [64]. Copyright 2013, Springer Nature. (b) Synthesis of poly(S-co-DiPhDY).

was prepared. During discharge, the disulfide bonds dissociate, yet the sulfides remain attached to the backbone [(Fig. 5(b)]. Crosslinkers can also be used to increase the sulfur content while maintaining structural stability in all states of charge.[70] For instance, Hawker and coworkers presented a sixfold symmetric C_6S_6 linker with a theoretical capacity of 610 mAh/g [Fig. 5(c)]. A cell fabricated with this cathode exhibited capacity retention of 98% after 200 cycles.[32]

Polymer sulfurization

Direct sulfurization of polymers is another method to prepare redoxmers with high sulfur content. Trofimov and coworkers demonstrated this sulfurization by mixing elemental sulfur with common polymers above 160 °C; in this reaction, the polysulfides are directly grafted on to the polymer backbone.[71] Wang and coworkers prepared a sulfurized polyacrylonitrile (SPAN) by heating polyacrylonitrile (PAN) and sulfur at 300 °C, in which PAN was simultaneously dehydrogenated and cyclized to obtain thio-amide and poly(sulfide) structures shown in Fig. 6(a).[72] Li_2S was found to be the sole discharge product [Fig. 6(b)] with negligible polysulfide shuttling.[73] To improve the conductivity of this cathode, Liu and coworkers developed a highly ordered mesoporous SPAN shown in Fig. 6(c).[33] This cathode was stable over 900 cycles at a rate of 2 C. The improved performance is attributed to the high specific surface that promotes electrolyte infusion and efficient ion transfer.

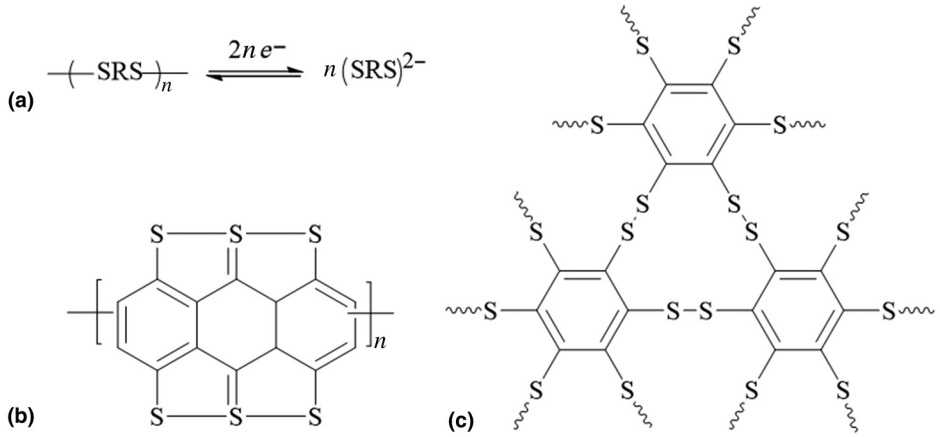


Figure 5. (a) Thiol–thiolate conversion. (b) Chemical structure of PABTP with active sulfur sidechains. (c) Chemical structure of C_6S_6-based cathode with high sulfur loadings.

https://doi.org/10.1557/mrc.2019.122 Published online by Cambridge University Press

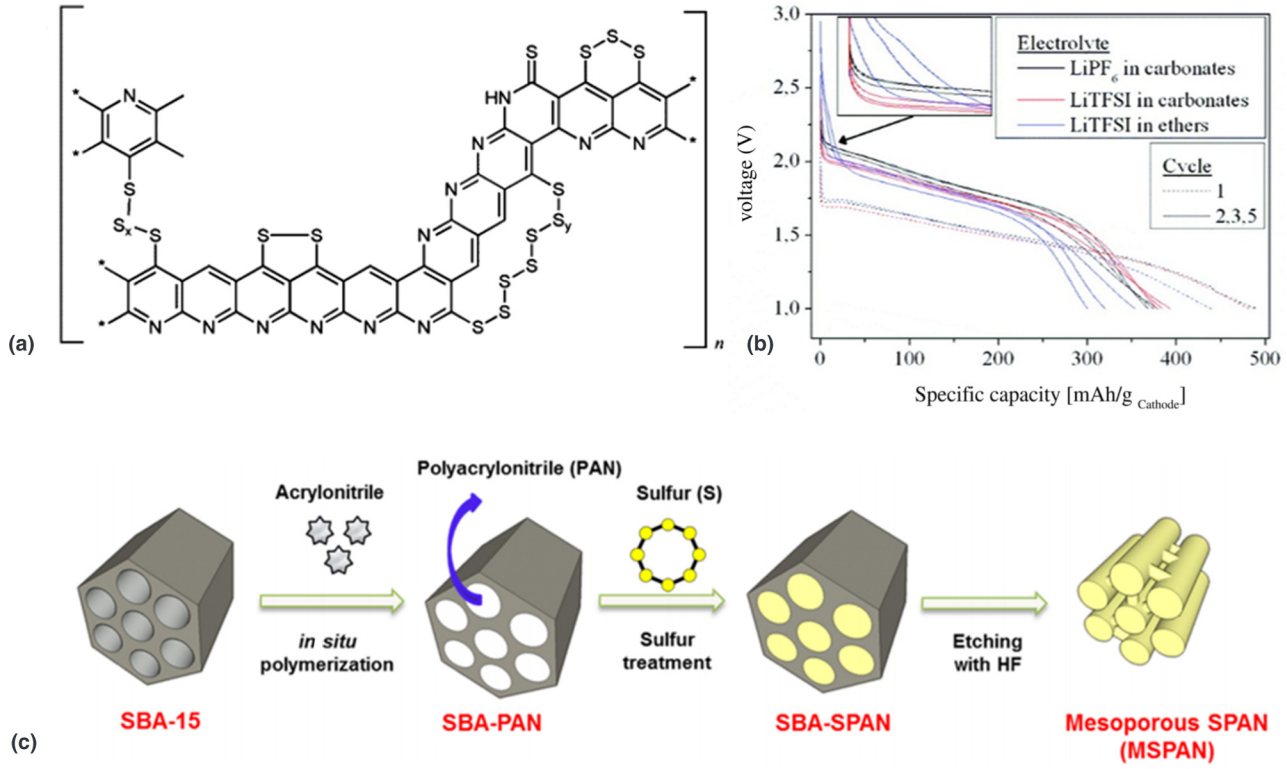


Figure 6. (a) Proposed structure of SPAN. Reproduced with permission from Ref. [72]. Copyright 2011, American Chemical Society. (b) Voltage-capacity profiles for SPAN cells in various electrolytes. (c) Synthesis of mesoporous SPAN using SBA-15 templates. Reproduced with permission from Ref. [33]. Copyright 2017, American Chemical Society.

Importantly, even if the redoxmers are not directly used for charge storage, they can still serve as charge transfer *mediators* that catalyze reactions involving lithium polysulfides. For example, polymeric 2,6-polyanthraquinone (PAQ) was shown to mediate redox reactions of sulfur species, thereby improving the cycling performance.[74]

Supercapacitors

Based on the mode of charge storage, SCs can be classified into pseudocapacitors and electric double-layer capacitors. To store charge, the pseudocapacitors rely on redox reactions of electrode materials (hence "pseudo" in their name, as they are not true capacitors), whereas electric double-layer capacitors store charge at the interface. In this review, we examine the use of redoxmers in the pseudocapacitors.

Redox polymer electrodes

To be useful in pseudocapacitors, the redoxmers need to be charged and discharged rapidly. Polymers with high electrical conductivity, such as poly(3,4-ethylenedioxythiophene) (PEDOT), polyaniline (PANI), polypyrrole (PPy), polyacetylene (PA), and polythiophene (PT), are the most common option for the conductive backbones; optimally, one needs both the high electrical conductivity *and* the high content of redox-active groups to store charge. Dichtel and coworkers introduced β-ketoenamine-linked 2D covalent organic frameworks (COFs) that exhibit fast reversible charging and excellent chemical stability in aqueous acids (which are typical electrolytes in such SCs). 2,6-Diaminoanthraquinone (DAAQ) was incorporated into the COFs as a redox-active pendant to obtain the capacitance of 48 ± 10 F/g with ~83% retention after 500 cycles.[75] Luscombe and coworkers designed a porous *n*-type hyperbranched polymer consisting of triphenylamine cores and NDI terminal units. The porosity of this material was tuned by varying the number of thiophene rings, and the electrode was stable after 500 cycles.[76]

Polymer/carbonaceous composite electrodes

Blending of redoxmers with conductive carbons and CNTs can be a convenient way to improve their performance. The key concern is to maintain electric contact between the two components throughout the cycle. Bachman et al. reported an electropolymerization method to prepare nanostructured pyrene derivatives based on oxygen-functionalized FWNTs (few-walled carbon nanotubes).[34] Functionalized pyrene molecules with a redox potential of ~3.5 V versus Li/Li^+ were conjugated to the chemically oxidized FWNTs. The poly-aminopyrene/FWNTs composite electrode delivered the specific capacity of 175 mAh/g and the average capacitance of 210 F/g. A power density of ~10 W/g was achieved with 85% capacity

https://doi.org/10.1557/mrc.2019.122 Published online by Cambridge University Press

retention over 10^4 cycles. Zhou et al. developed an electrochemical co-deposition method to obtain layered PPy/rGO/CNT and PEDOT/rGO/CNT structures on conductive glass (Fig. 7).[77] The CNTs in the bottom layer form the interconnected network that facilitates charge transfer. The composite electrode has high area-specific capacitance of 33.4 mF/cm^2 that lasts for >5000 cycles.[78] Duan's group reported a functionalized graphene hydrogel (FGH) obtained in a reaction of graphene oxide with hydroquinones that serve both as reducing agents *and* pendant groups in the FGH.[35] This material has a specific capacitance of 440 F/g, nearly one half of which comes from these hydroquinone pendants, with the capacity retention of 86% after 10^4 cycles.

All-redoxmer batteries

All-organic batteries offer low weight, mechanical flexibility, ease of processing, and improved sustainability. In 2018, Nishide and coworkers reported all-redoxmer LIB operating at 2.6 V with poly(vinyldibenzothiophenesulfone) anode and 2,2,6,6-tetramethylpiperidine-1-oxyl (TEMPO)-substituted poly(methacrylate) cathode [Fig. 8(a)],[36] with the initial discharge capacity of 540 mWh/g. Recently, the same group reported ultrathin (<1 μm) devices than can be attached to human skin.[79] The device has 100 nm thick poly-quinone anode and poly-TEMPO cathode that can be laterally stretched by 700% without deterioration of cycling performance; it is an impressive feat of engineering. Such designs are not limited to LMBs. Cao and coworkers reported an all-redoxmer sodium ion cell obtained by combining poly(aniline/*o*-nitroaniline) [P(AN-NA)] cathode with poly(anthraquinonyl sulfide) (PAQS) anode, and using a sodium ion-doped plastic crystal electrolyte.[80] Furthermore, one does not have to use two types of redoxmer materials. Zhang and coworkers explored a *symmetric* LIB with heterocyclic poly(quinone), poly(2,3-dithiino-1,4-benzoquinone) (PDB) as a bifunctional electrode[37] [Fig. 8(b)]. Using prelithiated PDB cathode and unlithiated PDB anode, they obtained a cell with the initial discharge capacity of 249 mAh/g at 20 mA/g and the specific energy of 276 Wh/kg. This excellent performance is attributed to the unique ladder-like structure of the polymer that provides a high density of redox units and ensures their electrochemical stability.

Conclusion and outlook

Despite their late coming on the scene, the redoxmers play an increasingly important role in the development of next-generation EES devices. No other class of materials serves in as many roles in so many devices. They can be used as electrodes, binders, electrolytes, and additives, in SCs and the batteries proper. The latter include LMBs, SMBs, MBs, Li–S batteries, and all-organic batteries. Due to limited space, we did not cover their other applications, such as their use as soluble active materials in redox flow batteries. Given this multiplicity of roles, one can be confident that the redoxmers will

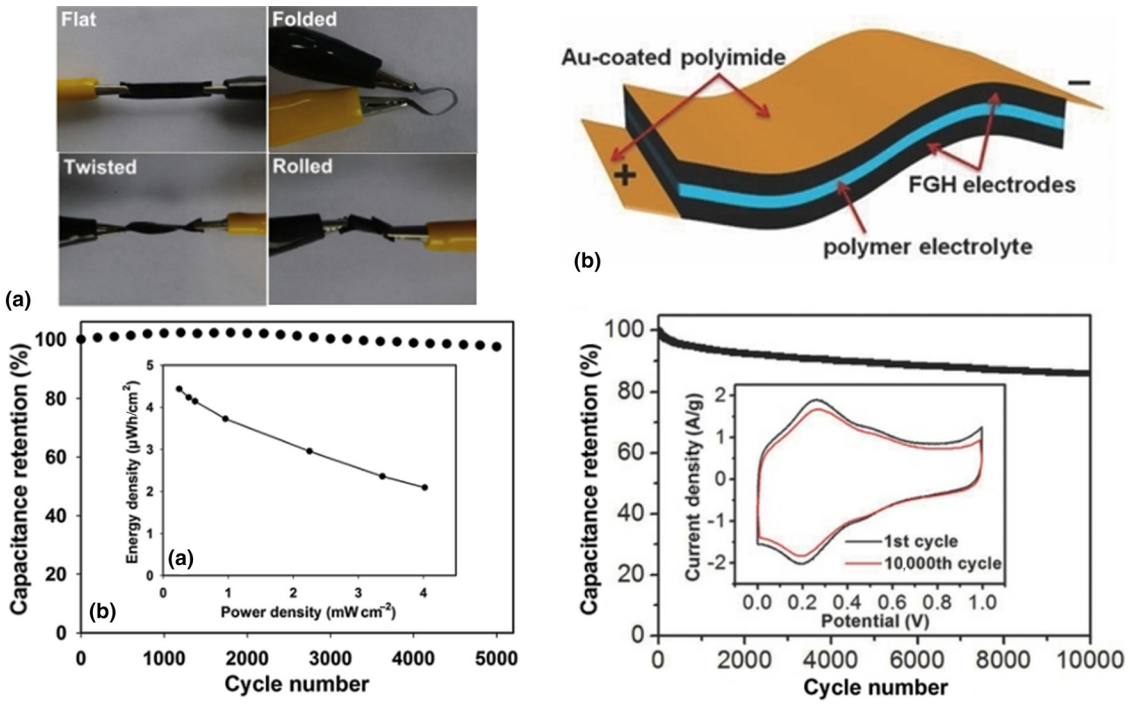


Figure 7. (a) Flexible SC based on CNT with the capacity retention data shown below. Reproduced with permission from Ref. [78]. Copyright 2016, Elsevier B.V. (b) Structure of FGH-based SC with the cycling voltammetry plot and capacity retention data shown below. Reproduced with permission from Ref. [35]. Copyright 2013, WILEY-VCH Verlag GmbH & Co. KGaA, Weinheim.

https://doi.org/10.1557/mrc.2019.122 Published online by Cambridge University Press

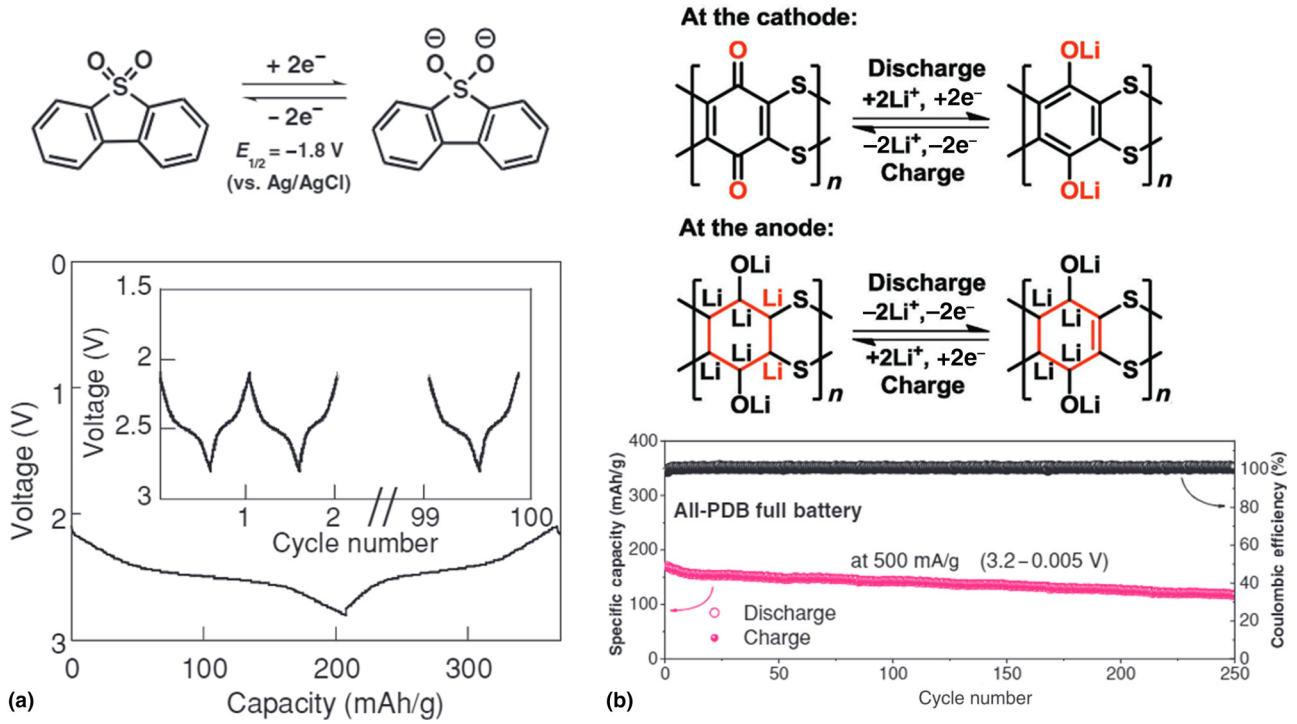


Figure 8. (a) Redox reaction of dibenzothiophenesulfone and voltage profile for the poly(vinyldibenzothiophenesulfone) electrode. Reproduced with permission from Ref. [36]. Copyright 2018, WILEY-VCH Verlag GmbH & Co. KGaA, Weinheim. (b) Proposed cycling mechanism and capacity retention for PDB. Reproduced with permission from Ref. [37]. Copyright 2018, WILEY-VCH Verlag GmbH & Co. KGaA, Weinheim.

become ubiquitous in commercial EES devices of the future. Still, there are two areas in which improvement is imperative.

(1) *The development of high energy density redoxmer-based electrodes*: A significant detriment of organic redoxmers is their relatively low energy density compared to the premier inorganic materials. Moreover, a lower electric conductivity of these organic redoxmers frequently requires a higher fraction of conductive particles in the electrode matrix, which further lowers the volumetric energy density of the composite electrode. Much improvement is needed to increase this energy density and also improve cycling stability at high and low rates.

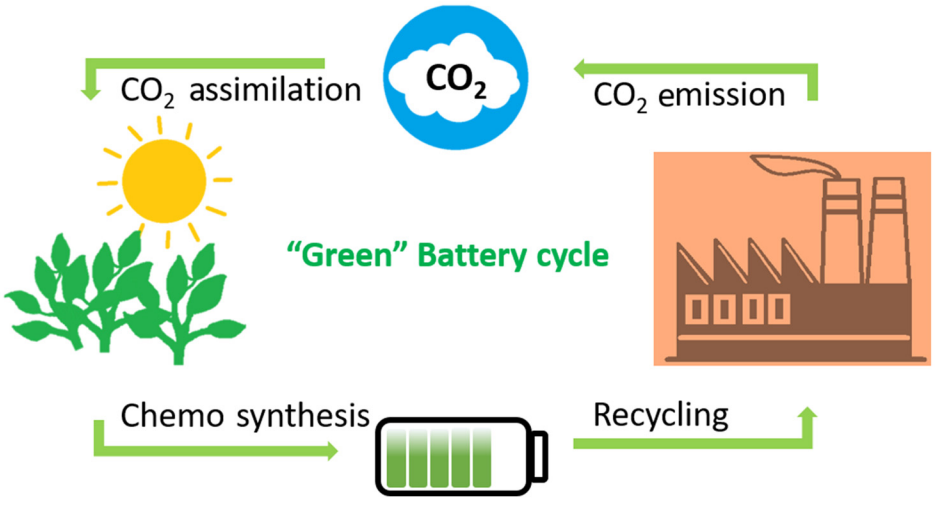


Figure 9. Schematic illustration of a cycle life of "green" Li metal batteries.

https://doi.org/10.1557/mrc.2019.122 Published online by Cambridge University Press

(2) *Sustainability and recyclability*: As LIBs are increasingly used for transportation and grid energy storage, recycling of such batteries emerged as a major concern. Hydrometallurgical processing,[81] thermal treatment,[82] and mechanical extraction[83] are all considered for industrial-scale recycling. However, even the best methods lead to incomplete recovery of valuable materials while generating hazardous waste. Given such realities, the global deployment of large-scale LIBs will strain the supply of inorganic materials.

Redoxmers are different in this respect as they consist of crustally abundant materials that are easy to recycle; some of these materials can even be naturally available (Fig. 9). To illustrate, Chen et al. developed a high-capacity $Li_xC_6O_6$ material from *myo*-inositol in biomass so that one can grow this material in fields and forests![84] As we have seen, polycarbonyls have emerged as a major cathode material; the monomers of such compounds are closely related to photosynthetic metabolites and can be obtained from plants.[85] After their use in the batteries, these polymers can be oxidized back to CO_2 and become taken by plants, in this way completing the cycle. Another striking example of "green" redoxmer chemistry was given by Theato and coworkers who prepared a cathode by copolymerization of S with vegetable oils.[86] Their Li–S cell delivered the initial capacity of 880 mA/g with the capacity retention of 63% after 100 cycles. These could be unimpressive metrics yet but, as Samuel Johnson famously quipped after seeing a dog walking on its hind legs, "it is not done well, but you are surprised to find it done at all." As our activity disturbs the environment, we need more surprises of this kind.

Acknowledgments

This work was supported as part of the Joint Center for Energy Storage Research, an Energy Innovation Hub funded by the U. S. Department of Energy, Office of Science, Basic Energy Sciences. The submitted manuscript has been created by UChicago Argonne, LLC, Operator of Argonne National Laboratory ("Argonne"). Argonne, a U.S. Department of Energy Office of Science laboratory, is operated under Contract No. DE-AC02-06CH11357.

References

1. L. Capuano: International Energy Outlook, 2018 (accessed 7 November).
2. T.M. Gür: Review of electrical energy storage technologies, materials and systems: challenges and prospects for large-scale grid storage. *Energ. Environ. Sci.* **11**, 2696–2767 (2018).
3. W. Wang, Q. Luo, B. Li, X. Wei, L. Li, and Z. Yang: Recent progress in redox flow battery research and development. *Adv. Funct. Mater.* **23**, 970–986 (2013).
4. Y. Liang, Z. Tao, and J. Chen: Organic electrode materials for rechargeable lithium batteries. *Adv. Energy Mater.* **2**, 742–769 (2012).
5. S. Muench, A. Wild, C. Friebe, B. Häupler, T. Janoschka, and U.S. Schubert: Polymer-based organic batteries. *Chem. Rev.* **116**, 9438–9484 (2016).
6. H. Zhang, M. Armand, and T. Rojo: Innovative polymeric materials for better rechargeable batteries: strategies from CIC Energigune. *J. Electrochem. Soc.* **166**, A679–A686 (2019).
7. Z. Song, Y. Qian, M.L. Gordin, D. Tang, T. Xu, M. Otani, H. Zhan, H. Zhou, and D. Wang: Polyanthraquinone as a reliable organic electrode for stable and fast lithium storage. *Angew. Chem. Int. Ed.* **54**, 13947–13951 (2015).
8. Y. Sasada, S.J. Langford, K. Oyaizu, and H. Nishide: Poly (norbornyl-NDIs) as a potential cathode-active material in rechargeable charge storage devices. *RSC Adv.* **6**, 42911–42916 (2016).
9. S. Maniam, K. Oka, and H. Nishide: *N*-Phenyl naphthalene diimide pendant polymer as a charge storage material with high rate capability and cyclability. *MRS Commun.* **7**, 967–973 (2017).
10. T.B. Schon, A.J. Tilley, E.L. Kynaston, and D.S. Seferos: Three-dimensional arylene diimide frameworks for highly stable lithium ion batteries. *ACS Appl. Mater. Inter.* **9**, 15631–15637 (2017).
11. H. Tokue, T. Murata, H. Agatsuma, H. Nishide, and K. Oyaizu: Charge–discharge with rocking-chair-type Li+ migration characteristics in a zwitterionic radical copolymer composed of TEMPO and trifluoromethanesulfonylimide with carbonate electrolytes for a high-rate Li-ion battery. *Macromolecules* **50**, 1950–1958 (2017).
12. T. Suga, H. Konishi, and H. Nishide: Photocrosslinked nitroxide polymer cathode-active materials for application in an organic-based paper battery. *Chem. Comm.* 1730–1732 (2007).
13. C. Karlsson, T. Suga, and H. Nishide: Quantifying TEMPO redox polymer charge transport toward the organic radical battery. *ACS Appl. Mater. Inter.* **9**, 10692–10698 (2017).
14. K. Koshika, N. Chikushi, N. Sano, K. Oyaizu, and H. Nishide: A TEMPO-substituted polyacrylamide as a new cathode material: an organic rechargeable device composed of polymer electrodes and aqueous electrolyte. *Green Chem.* **12**, 1573–1575 (2010).
15. G. Li, B. Zhang, J. Wang, H. Zhao, W. Ma, L. Xu, W. Zhang, K. Zhou, Y. Du, and G. He: Electrochromic poly(chalcogenoviologen)s as anode materials for high-performance organic radical lithium-ion batteries. *Angew. Chem. Int. Ed* **58**, 8468–8473 (2019).
16. N. Casado, G. Hernández, A. Veloso, S. Devaraj, D. Mecerreyes, and M. Armand: PEDOT radical polymer with synergetic redox and electrical properties. *ACS Macro Lett.* **5**, 59–64 (2016).
17. I. Aldalur, M. Martinez-Ibañez, M. Piszcz, H. Zhang, and M. Armand: Self-standing highly conductive solid electrolytes based on block copolymers for rechargeable all-solid-state lithium-metal batteries. *Batteries Supercaps* **1**, 149–159 (2018).
18. L. Xing, W. Li, C. Wang, F. Gu, M. Xu, C. Tan, and J. Yi: Theoretical investigations on oxidative stability of solvents and oxidative decomposition mechanism of ethylene carbonate for lithium ion battery use. *J. Phys. Chem. B* **113**, 16596–16602 (2009).
19. S. Grugeon, P. Jankowski, D. Cailleu, C. Forestier, L. Sannier, M. Armand, P. Johansson, and S. Laruelle: Towards a better understanding of vinylene carbonate derived SEI-layers by synthesis of reduction compounds. *J. Power Sources* **427**, 77–84 (2019).
20. G.-L. Xu, Q. Liu, K.K.S. Lau, Y. Liu, X. Liu, H. Gao, X. Zhou, M. Zhuang, Y. Ren, J. Li, M. Shao, M. Ouyang, F. Pan, Z. Chen, K. Amine, and G. Chen: Building ultraconformal protective layers on both secondary and primary particles of layered lithium transition metal oxide cathodes. *Nat. Energy* **4**, 484–494 (2019).
21. D. Zhou, Y. Chen, B. Li, H. Fan, F. Cheng, D. Shanmukaraj, T. Rojo, M. Armand, and G. Wang: A stable quasi-solid-state sodium–sulfur battery. *Angew. Chem.* **130**, 10325–10329 (2018).
22. E. Castillo-Martínez, J. Carretero-González, and M. Armand: Polymeric schiff bases as low-voltage redox centers for sodium-ion batteries. *Angew. Chem. Int. Ed.* **53**, 5341–5345 (2014).
23. Q. Zhao, R.R. Gaddam, D. Yang, E. Strounina, A.K. Whittaker, and X.S. Zhao: Pyromellitic dianhydride-based polyimide anodes for sodium-ion batteries. *Electrochim. Acta* **265**, 702–708 (2018).
24. T. Bančič, J. Bitenc, K. Pirnat, A. Kopač Lautar, J. Grdadolnik, A. Randon Vitanova, and R. Dominko: Electrochemical performance and redox mechanism of naphthalene-hydrazine diimide polymer as a cathode in magnesium battery. *J. Power Sources* **395**, 25–30 (2018).
25. A. Vizintin, J. Bitenc, A. Kopač Lautar, K. Pirnat, J. Grdadolnik, J. Stare, A. Randon-Vitanova, and R. Dominko: Probing electrochemical reactions in

https://doi.org/10.1557/mrc.2019.122 Published online by Cambridge University Press

organic cathode materials via in operando infrared spectroscopy. *Nat. Comm.* **9**, 661 (2018).
26. B. Pan, J. Huang, Z. Feng, L. Zeng, M. He, L. Zhang, J.T. Vaughey, M.J. Bedzyk, P. Fenter, Z. Zhang, A.K. Burrell, and C. Liao: Polyanthraquinone-based organic cathode for high-performance rechargeable magnesium-ion batteries. *Adv. Energy Mater.* **6**, 1600140 (2016).
27. H. Dong, Y. Liang, O. Tutusaus, R. Mohtadi, Y. Zhang, F. Hao, and Y. Yao: Directing Mg-storage chemistry in organic polymers toward high-energy Mg batteries. *Joule* **3**, 782–793 (2019).
28. A.G. Simmonds, J.J. Griebel, J. Park, K.R. Kim, W.J. Chung, V.P. Oleshko, J. Kim, E.T. Kim, R.S. Glass, C.L. Soles, Y.-E. Sung, K. Char, and J. Pyun: Inverse vulcanization of elemental sulfur to prepare polymeric electrode materials for Li–S batteries. *ACS Macro Lett.* **3**, 229–232 (2014).
29. P.T. Dirlam, A.G. Simmonds, T.S. Kleine, N.A. Nguyen, L.E. Anderson, A. O. Klever, A. Florian, P.J. Costanzo, P. Theato, M.E. Mackay, R.S. Glass, K. Char, and J. Pyun: Inverse vulcanization of elemental sulfur with 1,4-diphenylbutadiyne for cathode materials in Li–S batteries. *RSC Adv.* **5**, 24718–24722 (2015).
30. Y. Wei, X. Li, Z. Xu, H. Sun, Y. Zheng, L. Peng, Z. Liu, C. Gao, and M. Gao: Solution processible hyperbranched inverse-vulcanized polymers as new cathode materials in Li–S batteries. *Polym. Chem.* **6**, 973–982 (2015).
31. Z.J. Liu, L.B. Kong, Y.H. Zhou, and C.M. Zhan: Polyanthra[1,9,8-b,c,d,e][4,10,5-b,c,d,e]bis-[1,6,6a(6a-S) trithia]pentalene-active material for cathode of lithium secondary battery with unusually high specific capacity. *J. Power Sources* **161**, 1302–1306 (2006).
32. M.B. Preefer, B. Oschmann, C.J. Hawker, R. Seshadri, and F. Wudl: High sulfur content material with stable cycling in lithium-sulfur batteries. *Angew. Chem. Int. Ed.* **56**, 15118–15122 (2017).
33. Y. Liu, A.K. Haridas, K.-K. Cho, Y. Lee, and J.-H. Ahn: Highly ordered mesoporous sulfurized polyacrylonitrile cathode material for high-rate lithium sulfur batteries. *J. Phys. Chem. C* **121**, 26172–26179 (2017).
34. J.C. Bachman, R. Kavian, D.J. Graham, D.Y. Kim, S. Noda, D.G. Nocera, Y. Shao-Horn, and S.W. Lee: Electrochemical polymerization of pyrene derivatives on functionalized carbon nanotubes for pseudocapacitive electrodes. *Nat. Commun.* **6**, 7040 (2015).
35. Y. Xu, Z. Lin, X. Huang, Y. Wang, Y. Huang, and X. Duan: Functionalized graphene hydrogel-based high-performance supercapacitors. *Adv. Mater.* **25**, 5779–5784 (2013).
36. K. Oka, R. Kato, K. Oyaizu, and H. Nishide: Poly(vinyldibenzothiophene-sulfone): its redox capability at very negative potential toward an all-organic rechargeable device with high-energy density. *Adv. Funct. Mater.* **28**, 1805858 (2018).
37. J. Xie, Z.L. Wang, Z.C.J. Xu, and Q.C. Zhang: Toward a high-performance all-plastic full battery with a single organic polymer as both cathode and anode. *Adv. Energy Mater.* **8**, 1703509 (2018).
38. K. Nakahara, S. Iwasa, M. Satoh, Y. Morioka, J. Iriyama, M. Suguro, and E. Hasegawa: Rechargeable batteries with organic radical cathodes. *Chem. Phys. Lett.* **359**, 351–354 (2002).
39. H. Zhang, G.G. Eshetu, X. Judez, C. Li, L.M. Rodriguez-Martínez, and M. Armand: Electrolyte additives for lithium metal anodes and rechargeable lithium metal batteries: progress and perspectives. *Angew. Chem. Int. Ed.* **57**, 15002–15027 (2018).
40. A.T. Appapillai, A.N. Mansour, J. Cho, and Y. Shao-Horn: Microstructure of $LiCoO_2$ with and without "$AlPO_4$" nanoparticle coating: combined STEM and XPS studies. *Chem. Mater.* **19**, 5748–5757 (2007).
41. X. Li, J. Liu, M.N. Banis, A. Lushington, R. Li, M. Cai, and X. Sun: Atomic layer deposition of solid-state electrolyte coated cathode materials with superior high-voltage cycling behavior for lithium ion battery application. *Energ. Environ. Sci.* **7**, 768–778 (2014).
42. K.-S. Lee, S.-T. Myung, K. Amine, H. Yashiro, and Y.-K. Sun: Dual functioned BiOF-coated $Li[Li_{0.1}Al_{0.05}Mn_{1.85}]O_4$ for lithium batteries. *J. Mater. Chem.* **19**, 1995–2005 (2009).
43. P. Yan, J. Zheng, T. Chen, L. Luo, Y. Jiang, K. Wang, M. Sui, J.-G. Zhang, S. Zhang, and C. Wang: Coupling of electrochemically triggered thermal and mechanical effects to aggravate failure in a layered cathode. *Nat. Commun.* **9**, 2437 (2018).
44. M.D. Slater, D. Kim, E. Lee, and C.S. Johnson: Sodium-ion batteries. *Adv. Funct. Mater.* **23**, 947–958 (2013).
45. P. Canepa, S.-H. Bo, G. Sai Gautam, B. Key, W.D. Richards, T. Shi, Y. Tian, Y. Wang, J. Li, and G. Ceder: High magnesium mobility in ternary spinel chalcogenides. *Nat. Chem.* **8**, 1759 (2017).
46. J.T. Incorvati, L.F. Wan, B. Key, D. Zhou, C. Liao, L. Fuoco, M. Holland, H. Wang, D. Prendergast, K.R. Poeppelmeier, and J.T. Vaughey: Reversible magnesium intercalation into a layered oxyfluoride cathode. *Chem. Mater.* **28**, 17–20 (2016).
47. C. Yu, C. Wang, X. Liu, X. Jia, S. Naficy, K. Shu, M. Forsyth, and G.G. Wallace: A cytocompatible robust hybrid conducting polymer hydrogel for use in a magnesium battery. *Adv. Mater.* **28**, 9349–9355 (2016).
48. X. Jia, C. Wang, V. Ranganathan, B. Napier, C. Yu, Y. Chao, M. Forsyth, F. G. Omenetto, D.R. MacFarlane, and G.G. Wallace: A biodegradable thin-film magnesium primary battery using silk fibroin–ionic liquid polymer electrolyte. *ACS Energy Lett.* **2**, 831–836 (2017).
49. P.G. Bruce, S.A. Freunberger, L.J. Hardwick, and J.-M. Tarascon: Li–O_2 and Li–S batteries with high energy storage. *Nat. Mater.* **11**, 19 (2011).
50. B.C. Melot and J.M. Tarascon: Design and preparation of materials for advanced electrochemical storage. *Acc. Chem. Rev.* **46**, 1226–1238 (2013).
51. X. Ji and L.F. Nazar: Advances in Li–S batteries. *J. Mater. Chem.* **20**, 9821–9826 (2010).
52. K. Kang, Y.S. Meng, J. Bréger, C.P. Grey, and G. Ceder: Electrodes with high power and high capacity for rechargeable lithium batteries. *Science* **311**, 977–980 (2006).
53. Y.V. Mikhaylik and J.R. Akridge: Polysulfide shuttle study in the Li/S battery system. *J. Electrochem. Soc.* **151**, A1969–A1976 (2004).
54. X. Liang, C. Hart, Q. Pang, A. Garsuch, T. Weiss, and L.F. Nazar: A highly efficient polysulfide mediator for lithium–sulfur batteries. *Nat. Commun.* **6**, 5682 (2015).
55. W. Xu, J. Wang, F. Ding, X. Chen, E. Nasybulin, Y. Zhang, and J.-G. Zhang: Lithium metal anodes for rechargeable batteries. *Energ. Environ. Sci.* **7**, 513–537 (2014).
56. B. Liu, J.-G. Zhang, and W. Xu: Advancing lithium metal batteries. *Joule* **2**, 833–845 (2018).
57. X. Yu and A. Manthiram: Electrode–electrolyte interfaces in lithium-based batteries. *Energ. Environ. Sci.* **11**, 527–543 (2018).
58. X. Ji, K.T. Lee, and L.F. Nazar: A highly ordered nanostructured carbon–sulphur cathode for lithium–sulphur batteries. *Nat. Mater.* **8**, 500 (2009).
59. H. Wei, E.F. Rodriguez, A.S. Best, A.F. Hollenkamp, D. Chen, and R.A. Caruso: Chemical bonding and physical trapping of sulfur in mesoporous magnéli Ti_4O_7 microspheres for high-performance Li–S battery. *Adv. Energy Mater.* **7**, 1601616 (2017).
60. D. Lei, K. Shi, H. Ye, Z. Wan, Y. Wang, L. Shen, B. Li, Q.-H. Yang, F. Kang, and Y.-B. He: Progress and perspective of solid-state lithium–sulfur batteries. *Adv. Funct. Mater.* **28**, 1707570 (2018).
61. M.J. Lacey, F. Jeschull, K. Edström, and D. Brandell: Porosity blocking in highly porous carbon black by PVdF binder and its implications for the Li–S system. *J. Phys. Chem. C* **118**, 25890–25898 (2014).
62. Z. Cheng, H. Pan, H. Zhong, Z. Xiao, X. Li, and R. Wang: Porous organic polymers for polysulfide trapping in lithium–sulfur batteries. *Adv. Funct. Mater.* **28**, 1707597 (2018).
63. H. Schneider, A. Garsuch, A. Panchenko, O. Gronwald, N. Janssen, and P. Novák: Influence of different electrode compositions and binder materials on the performance of lithium–sulfur batteries. *J. Power Sources* **205**, 420–425 (2012).
64. W.J. Chung, J.J. Griebel, E.T. Kim, H. Yoon, A.G. Simmonds, H.J. Ji, P.T. Dirlam, R.S. Glass, J.J. Wie, N.A. Nguyen, B.W. Guralnick, J. Park, Á Somogyi, P. Theato, M.E. Mackay, Y.-E. Sung, K. Char, and J. Pyun: The use of elemental sulfur as an alternative feedstock for polymeric materials. *Nat. Chem.* **5**, 518 (2013).
65. J.J. Griebel, G. Li, R.S. Glass, K. Char, and J. Pyun: Kilogram scale inverse vulcanization of elemental sulfur to prepare high capacity polymer electrodes for Li-S batteries. *J. Polym. Sci. Pol. Chem.* **53**, 173–177 (2015).
66. B. Oschmann, J. Park, C. Kim, K. Char, Y.-E. Sung, and R. Zentel: Copolymerization of polythiophene and sulfur to improve the electrochemical performance in lithium–sulfur batteries. *Chem. Mater.* **27**, 7011–7017 (2015).

https://doi.org/10.1557/mrc.2019.122 Published online by Cambridge University Press

67. F. Wu, S. Chen, V. Srot, Y. Huang, S.K. Sinha, P.A. van Aken, J. Maier, and Y. Yu: A sulfur–limonene-based electrode for lithium–sulfur batteries: high-performance by self-protection. *Adv. Mater.* **30**, 1706643 (2018).
68. H. Berk, B. Balci, S. Ertan, M. Kaya, and A. Cihaner: Functionalized polysulfide copolymers with 4-vinylpyridine via inverse vulcanization. *Mater. Today Commun.* **19**, 336–341 (2019).
69. M.M. Doeff, M.M. Lerner, S.J. Visco, and L.C. De Jonghe: The use of polydisulfides and copolymeric disulfides in the Li/PEO/SRPE battery system. *J. Electrochem. Soc.* **139**, 2077–2081 (1992).
70. H. Kim, J. Lee, H. Ahn, O. Kim, and M.J. Park: Synthesis of three-dimensionally interconnected sulfur-rich polymers for cathode materials of high-rate lithium–sulfur batteries. *Nat. Commun.* **6**, 7278 (2015).
71. B.A. Trofimov, A.M. Vasil'tsov, O.V. Petrova, A.I. Mikhaleva, G.F. Myachina, S.A. Korzhova, T.A. Skotheim, Y.V. Mikhailik, and T.I. Vakul'skaya: Sulfurization of polymers. 6. Poly(vinylene polysulfide), poly(thienothiophene), and related structures from polyacetylene and elemental sulfur. *Russ. Chem. Bull.* **51**, 1709–1714 (2002).
72. J. Fanous, M. Wegner, J. Grimminger, Ä Andresen, and M.R. Buchmeiser: Structure-related electrochemistry of sulfur-poly(acrylonitrile) composite cathode materials for rechargeable lithium batteries. *Chem. Mater.* **23**, 5024–5028 (2011).
73. S. Wei, L. Ma, K.E. Hendrickson, Z. Tu, and L.A. Archer: Metal–sulfur battery cathodes based on PAN–sulfur composites. *J. Am. Chem. Soc.* **137**, 12143–12152 (2015).
74. K.-C. Lau, I.A. Shkrob, N.L. Dietz Rago, J.G. Connell, D. Phelan, B. Hu, L. Zhang, Z. Zhang, and C. Liao: Improved performance through tight coupling of redox cycles of sulfur and 2,6-polyanthraquinone in lithium–sulfur batteries. *J. Mater. Chem. A* **5**, 24103–24109 (2017).
75. C.R. DeBlase, K.E. Silberstein, T.-T. Truong, H.D. Abruña, and W.R. Dichtel: β-Ketoenamine-linked covalent organic frameworks capable of pseudocapacitive energy storage. *J. Am. Chem. Soc.* **135**, 16821–16824 (2013).
76. D.F. Zeigler, S.L. Candelaria, K.A. Mazzio, T.R. Martin, E. Uchaker, S.-L. Suraru, L.J. Kang, G. Cao, and C.K. Luscombe: N-Type hyperbranched polymers for supercapacitor cathodes with variable porosity and excellent electrochemical stability. *Macromolecules* **48**, 5196–5203 (2015).
77. H. Zhou, X. Zhi, and H.-J. Zhai: Promoted supercapacitive performances of electrochemically synthesized poly(3,4-ethylenedioxythiophene) incorporated with manganese dioxide. *J. Mater. Sci. Mater. Elect.* **29**, 3935–3942 (2018).
78. H. Zhou, H.-J. Zhai, and G. Han: Superior performance of highly flexible solid-state supercapacitor based on the ternary composites of graphene oxide supported poly(3,4-ethylenedioxythiophene)-carbon nanotubes. *J. Power Sources* **323**, 125–133 (2016).
79. K. Hatakeyama-Sato, H. Wakamatsu, K. Yamagishi, T. Fujie, S. Takeoka, K. Oyaizu, and H. Nishide: Ultrathin and stretchable rechargeable devices with organic polymer nanosheets conformable to skin surface. *Small* **15**, 1805296 (2019).
80. X. Zhu, R. Zhao, W. Deng, X. Ai, H. Yang, and Y. Cao: An all-solid-state and all-organic sodium-ion battery based on redox-active polymers and plastic crystal electrolyte. *Electrochim. Acta* **178**, 55–59 (2015).
81. Y. Weng, S. Xu, G. Huang, and C. Jiang: Synthesis and performance of Li $[(Ni_{1/3}Co_{1/3}Mn_{1/3})_{1-x}Mg_x]O_2$ prepared from spent lithium ion batteries. *J. Hazard. Mater.* **246–247**, 163–172 (2013).
82. Y. Yang, G. Huang, S. Xu, Y. He, and X. Liu: Thermal treatment process for the recovery of valuable metals from spent lithium-ion batteries. *Hydrometallurgy* **165**, 390–396 (2016).
83. T. Zhang, Y. He, F. Wang, L. Ge, X. Zhu, and H. Li: Chemical and process mineralogical characterizations of spent lithium-ion batteries: an approach by multi-analytical techniques. *Waste Manage.* **34**, 1051–1058 (2014).
84. H. Chen, M. Armand, G. Demailly, F. Dolhem, P. Poizot, and J.-M. Tarascon: From biomass to a renewable $LiXC_6O_6$ organic electrode for sustainable Li-ion batteries. *ChemSusChem* **1**, 348–355 (2008).
85. M. Armand, and J.M. Tarascon: Building better batteries. *Nature* **451**, 652 (2008).
86. A. Hoefling, Y.J. Lee, and P. Theato: Sulfur-based polymer composites from vegetable oils and elemental sulfur: a sustainable active material for Li–S batteries. *Macromol. Chem. Phys.* **218**, 1600303 (2017).

https://doi.org/10.1557/mrc.2019.122 Published online by Cambridge University Press